Scientia Iranica, Vol. 10, No. 1, pp 74–83

SCIENTIA
IRANICA

3-D Thin Layer Navier-Stokes Solution of Supersonic Turbulent Flow

M.M. Alishahi*, H. Emdad[1] and O. Abouali[1]

In this research, a 3-D Thin Layer Navier-Stokes (TLNS) code is developed. This code consists of several numerical algorithms for space and time discretization, together with appropriate turbulence modeling. The Roe method is used for the discretization of inviscid terms and the central scheme for viscous terms. The explicit time marching technique is applied, based on finite volume space discretization. This code can be employed in the range of laminar and turbulent flow. It is validated for a supersonic flow with Mach number 3 around a tangent-ogive with incidence angles of 6° and a secant-ogive with incidence angles of 10°. The circumferential pressure distribution is compared with experimental and Euler code results and the results of TLNS are acceptable. The cross-sectional Mach number contours are also presented. In addition to an outer shock, a cross-flow shock wave is captured in the case of a 10° angle of incidence.

INTRODUCTION

One of the most important aims of CFD research is to determine the complicated 3-D flow fields around flying objects. Before progress of digital computers, analytical and experimental methods were the only means available for resolving fluid dynamic problems.

It is obvious that the Euler or Navier-Stokes equations do not have analytical solutions except for very simple geometries. Fortunately, the progress of digital computers throughout the last decades, has brought about the opportunity of solving these equations numerically.

The methods for the solution of Euler equations are categorized in two main groups. The first one is the central differencing scheme. Lax-Wendrof [1] and MacCormac [2] methods belong to this group. Using this method, a programming task is made easy but one needs dissipative terms to capture shock waves. These artificial viscous terms are case dependent and determined via trial and error. Therefore, the generality of these methods is limited. The second category is based on an upwinding approach. Upwinding methods model the physical phenomenon of flow in a better way compared with the central differencing method. The type of discretization is selected depending on the propagation direction of information in the flow-field. This direction is related to the sign of the eigenvalues of Jacobian matrixes. In these methods, solution of the Reimann problem (one-dimensional shock tube problem) is implemented to determine the fluxes of the Euler equations. These methods capture the shock waves properly and do not need dissipative terms, but they are more time-consuming. Gudonov [3], Osher [4] and Roe [5] methods belong to this category. The solution of 3-D Navier-Stokes equations for compressible flow is very time-consuming and problems involving these equations are usually solved using supercomputers [6,7]. Fortunately, it is possible to solve some reduced forms of the Navier-Stokes equations in many situations. In most of these cases, viscous derivatives in the streamwise direction are negligible and can be left out of Navier-Stokes equations. After omitting these terms, the steady state forms of the resulted equations called Parabolized Navier-Stokes (PNS) are obtained. Using PNS, the run-time and necessary memory are reduced but the application of these equations is limited to supersonic flow with small streamwise pressure gradient and without streamwise separation [8,9]. Another set of reduced forms of the Navier-Stokes equations are Thin Layer Navier-Stokes (TLNS) equations. In this case, time derivative terms are not dropped out in comparison with the PNS equations.

In this investigation, a 3-D TLNS code is developed. The Roe method is used to discretize the inviscid terms [10] and central differencing for the

*. *Corresponding Author, Department of Mechanical Engineering, Shiraz University, Shiraz, I.R. Iran.*

1. *Department of Mechanical Engineering, Shiraz University, Shiraz, I.R. Iran.*

viscous terms. Time derivative terms are discretized with the Explicit technique. The Baldwin-Lomax model [11] and Degani-Schiff [12] modifications are used for turbulence modeling. The algorithm is based on a finite volume approach. The code is validated for two test cases. The first is a turbulent supersonic flow with Mach number 3 on a tangent-ogive cylinder at an incidence angle of 6°and the second is the same flow on a secant-ogive with an incidence angle of 10°. The addition of an implicit technique to the code and matching it with a PNS code [9] are currently being carried out and the results will be presented in the near future.

GOVERNING EQUATIONS

Navier-Stokes equations in Cartesian coordinates, in the conservative form are:

$$Q_t + (E - E_v)_x + (F - F_v)_y + (G - G_v)_z = 0 \tag{1}$$

$$Q = \begin{bmatrix} e \\ \rho \\ \rho u \\ \rho v \\ \rho w \end{bmatrix}, \quad E = \begin{bmatrix} (e+p)u \\ \rho u \\ \rho u^2 + p \\ \rho uv \\ \rho uw \end{bmatrix},$$

$$F = \begin{bmatrix} (e+p)v \\ \rho u \\ \rho uv \\ \rho v^2 + p \\ \rho wv \end{bmatrix}, \quad G = \begin{bmatrix} (e+p)w \\ \rho w \\ \rho uw \\ \rho vw \\ \rho w^2 + p \end{bmatrix}, \tag{2}$$

$$E_v = \begin{bmatrix} u\tau_{xx} + v\tau_{xy} + w\tau_{xz} - q_x \\ 0 \\ \tau_{xx} \\ \tau_{xy} \\ \tau_{xz} \end{bmatrix},$$

$$F_v = \begin{bmatrix} u\tau_{yx} + v\tau_{yy} + w\tau_{yz} - q_y \\ 0 \\ \tau_{yx} \\ \tau_{yy} \\ \tau_{yz} \end{bmatrix},$$

$$G_v = \begin{bmatrix} u\tau_{zx} + v\tau_{zy} + w\tau_{zz} - q_z \\ 0 \\ \tau_{zx} \\ \tau_{zy} \\ \tau_{zz} \end{bmatrix}, \tag{3}$$

in which:

$$e = \frac{p}{\gamma - 1} + \frac{\rho}{2}(u^2 + v^2 + w^2),$$

$$\tau_{xx} = \frac{2}{3}\mu\left(2\frac{\partial u}{\partial x} - \frac{\partial v}{\partial y} - \frac{\partial w}{\partial z}\right),$$

$$\tau_{yy} = \frac{2}{3}\mu\left(2\frac{\partial v}{\partial y} - \frac{\partial u}{\partial x} - \frac{\partial w}{\partial z}\right),$$

$$\tau_{zz} = \frac{2}{3}\mu\left(2\frac{\partial w}{\partial z} - \frac{\partial u}{\partial x} - \frac{\partial v}{\partial y}\right),$$

$$\tau_{xy} = \tau_{yx} = \mu\left(\frac{\partial u}{\partial y} + \frac{\partial v}{\partial x}\right),$$

$$\tau_{yz} = \tau_{zy} = \mu\left(\frac{\partial v}{\partial z} + \frac{\partial w}{\partial y}\right),$$

$$\tau_{xz} = \tau_{zx} = \mu\left(\frac{\partial u}{\partial z} + \frac{\partial w}{\partial x}\right),$$

$$q_x = -K\frac{\partial T}{\partial x}, \quad q_y = -K\frac{\partial T}{\partial y}, \quad q_z = -K\frac{\partial T}{\partial z},$$

$$\mu = \mu_L + \mu_t, \quad K = K_L + K_t. \tag{4}$$

The laminar coefficients of viscosity and thermal conductivity, μ_L and K_L, are related to the thermodynamic variables using the kinetic theory. Sutherland's formula for viscosity is given by:

$$\mu = C_1\frac{T^{3/2}}{T + C_2}, \tag{5}$$

where C_1 and C_2 are constants for a given gas. For air at moderate temperature, $C_1 = 1.458\times10^{-6}$ kg/msk$^{1/2}$ and $C_2 = 110.4$ k. The Prandtl number Pr $= \frac{C_p\mu}{k}$ is often used to determine the coefficient of thermal conductivity. μ_t and K_t will be defined later in this paper.

Equation 1 can be expressed in terms of generalized orthogonal curvilinear coordinates system, as:

$$\tilde{Q}_t + (\tilde{E} - \tilde{E}_v)_\xi + (\tilde{F} - \tilde{F}_v)_\eta + (\tilde{G} - \tilde{G}_v)_\zeta = 0, \tag{6}$$

$$\tilde{Q} = \frac{Q}{J},$$

$$\tilde{E} = \frac{\xi_x}{J}E + \frac{\xi_y}{J}F + \frac{\xi_z}{J}G,$$

$$\tilde{E}_v = \frac{\xi_x}{J}E_v + \frac{\xi_y}{J}F_v + \frac{\xi_z}{J}G_v,$$

$$\tilde{F} = \frac{\eta_x}{J}E + \frac{\eta_y}{J}F + \frac{\eta_z}{J}G,$$

$$\tilde{F}_v = \frac{\eta_x}{J}E_v + \frac{\eta_y}{J}F_v + \frac{\eta_z}{J}G_v,$$

$$\tilde{G} = \frac{\zeta_x}{J}E + \frac{\zeta_y}{J}F + \frac{\zeta_z}{J}G,$$

$$\tilde{G}_v = \frac{\zeta_x}{J}E_v + \frac{\zeta_y}{J}F_v + \frac{\zeta_z}{J}G_v, \tag{7}$$

in which J is the Jacobian of the transformation.

The thin layer approximation is now applied to the transformed Navier-Stokes equations. This

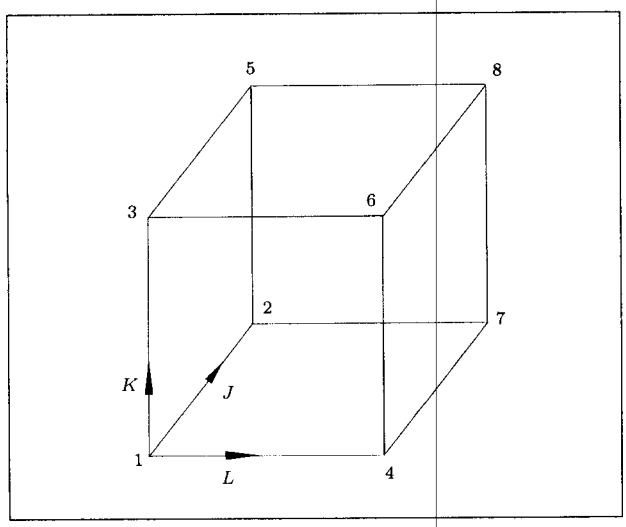

Figure 1. Computational volume cell.

approximation allows one to drop out all viscous terms containing partial derivatives, with respect to ξ and ζ, where η is generally perpendicular to walls.

The resulting thin layer equations may be written as:

$$\widetilde{Q}_t + \widetilde{E}_\xi + (\widetilde{F} - \widetilde{F}_v)_\eta + \widetilde{G}_\zeta = 0. \tag{8}$$

Equation 8 may be expressed in the semi-discrete conservation form given by:

$$\begin{aligned}(\hat{Q}_{j,k,l})_\tau &+ (\hat{E}_{j+1/2,k,l} - \hat{E}_{j-1/2,k,l}) \\ &+ \left((\hat{F} - \hat{F}_v)_{j,k+1/2,l} - (\hat{F} - \hat{F}_v)_{j,k-1/2,l}\right) \\ &+ (\hat{G}_{j,k,l+1/2} - \hat{G}_{j,k,l-1/2}) = 0,\end{aligned} \tag{9}$$

where $\hat{E}, \hat{F}, \hat{G}$ are the numerical fluxes at the bounding sides of the cell (Figure 1).

Equation 9 can be considered as a finite volume discretization of the continuity, momentum and energy equations, if it is assumed that:

$$\hat{Q}_{j,k,l} = QV_{j,k,l},$$

where V is the volume of the cell and:

$$\left(\frac{\xi_{x,y,z}}{J}\right)_{j+1/2}, \left(\frac{\eta_{x,y,z}}{J}\right)_{k+1/2}, \left(\frac{\zeta_{x,y,z}}{J}\right)_{j+1/2},$$

are components of the normal to the surface of the element.

COMPUTATION OF CELL VOLUME

To compute the cell volume, the cell is considered as a sum of six tetrahedrons.

$$\begin{aligned}V = &V^{tet}(1,2,5,8) + V^{tet}(1,2,8,7) + V^{tet}(1,3,8,5) \\ &+ V^{tet}(1,4,8,7) + V^{tet}(1,4,8,6) + V^{tet}(1,3,6,8),\end{aligned} \tag{10}$$

where the volume of tetrahedrons, having vertices a, b, c, d, are evaluated from:

$$\begin{aligned}V^{tet}(a,b,c,d) = &\\ &|x_a[y_b(z_c - z_d) - y_c(z_b - z_d) + y_d(z_d - z_c)] \\ &- x_b[y_a(z_c - z_d) - y_c(z_a - z_d) + y_d(z_a - z_c)] \\ &+ x_c[y_a(z_b - z_d) - y_b(z_a - z_d) + y_d(z_a - z_b)] \\ &- x_d[y_a(z_b - z_c) - y_b(z_a - z_c) + y_c(z_a - z_b)]|/6.\end{aligned} \tag{11}$$

COMPUTATION OF CELL-FACE METRICES (NORMALS)

The cell-face normals, having vertices a, b, c, d, are evaluated as:

$$\begin{aligned}n_x(a,b,c,d) =&(dy_{ba}dz_{cb} - dy_{cb}dz_{ba})/2 \\ &+ (dy_{dc}dz_{ad} - dy_{ad}dz_{dc})/2, \\ n_y(a,b,c,d) =&(dz_{ba}dx_{cb} - dz_{cb}dx_{ba})/2 \\ &+ (dz_{dc}dx_{ad} - dx_{ad}dx_{dc})/2, \\ n_z(a,b,c,d) =&(dx_{ba}dy_{cb} - dx_{cb}dy_{ba})/2 \\ &+ (dx_{dc}dy_{ad} - dx_{ad}dy_{dc})/2,\end{aligned} \tag{12}$$

in which $ds_{12} = s_1 - s_2$.

NUMERICAL INVISCID FLUXES (ROE APPROXIMATE RIEMANN SOLVER)

The Roe method is used for the calculation of the fluxes. So Equation 7 may be condensed to:

$$\widetilde{E}, \widetilde{F}, \widetilde{G} = f(Q, n_x, n_y, n_z) = f(Q, N). \tag{13}$$

The Jacobian matrix of the flux, f, with respect to Q, can be denoted by $\frac{\partial f}{\partial Q}$. The eigenvalues of the Jacobian matrix are shown by λ_i and the corresponding left and right eigenvectors by ℓ^i and r^i [13].

The left eigenvectors matrix is formed by left eigenvectors as rows and the right eigenvectors matrix is organized by right eigenvectors as a column.

In the Roe approach, the cell interface, values of density, velocity and enthalpy $\{h = \frac{\gamma p}{[(\gamma-1)\rho]} + \frac{(u^2+v^2+w^2)}{2}\}$ are computed using a special averaging procedure:

$$\begin{aligned}\rho_{m+1/2} &= \sqrt{\rho_m}\sqrt{\rho_{m+1}}, \\ (u,v,w)_{m+1/2} &= \frac{(u,v,w)_{m+1}\sqrt{\rho_{m+1}} + (u,v,w)_m\sqrt{\rho_m}}{\sqrt{\rho_{m+1}} + \sqrt{\rho_m}}, \\ h_{m+1/2} &= \frac{h_{m+1}\sqrt{\rho_{m+1}} + h_m\sqrt{\rho_m}}{\sqrt{\rho_{m+1}} + \sqrt{\rho_m}},\end{aligned} \tag{14}$$

where $m = j$ or k or l and speed of sound may be computed by:

$$C_{m+1/2} = \sqrt{\{h_{m+1/2} - (u^2 + v^2 + w^2)\}(\gamma - 1)}. \tag{15}$$

The formula for eigenvalues and eigenvector matrices are now presented.

Defining the contravariant velocity by $\overline{U} = n_x u + n_y v + n_z w$, eigenvalues are determined as:

$$\lambda^1 = \overline{U} - c\sqrt{n_x^2 + n_y^2 + n_z^2},$$
$$\lambda^{2,3,4} = \overline{U},$$
$$\lambda^5 = \overline{U} + c\sqrt{n_x^2 + n_y^2 + n_z^2}. \tag{16}$$

At each cell face, the positive and negative projections of the eigenvalues may be defined by:

$$\lambda^{i\pm} = \frac{(\lambda^i_{m+1/2} \pm |\lambda^i_{m+1/2}|)}{2} \quad i = 1, \cdots, 5. \tag{17}$$

To avoid expansion shock, only at sonic rarefaction's $[\lambda^i(U_m) < 0 < \lambda^i(U_{m+1})]$ equations are modified as:

$$\lambda^{i\pm}_{m+1/2} = \lambda^{i\pm}_{m+1/2} \pm \frac{[\lambda^i(U_{m+1}) - \lambda^i(U_m)]}{4}. \tag{18}$$

Defining $\hat{n}_{x,y,z} = \frac{n_{x,y,z}}{\sqrt{n_x^2+n_y^2+n_z^2}}$ and $\theta = (u^2+v^2+w^2)/2$, the left and right eigenvectors are presented in Table 1.

Now, the equation for calculating the first order upwind flux is defined as:

$$\begin{aligned} f_{m+1/2} &= 1/2[f(Q_{m+1}, N_{m+1/2}) + f(Q_m, N_{m+1/2})] \\ &\quad - 1/2\Big[\sum_i (\lambda^{i+}_{m+1/2} - \lambda^{i-}_{m+1/2})\ell^i_{m+1/2} \\ &\qquad (Q_{m+1} - Q_m) r^i_{m+1/2}\Big] \\ &= f(Q_m, N_{m+1/2}) = \sum_i \lambda^{i-}_{m+1/2} \alpha^i r^i_{m+1/2} \\ &= f + df^{i-} \\ &= f(Q_{m+1}, N_{m+1/2}) - \sum_i \lambda^{i+}_{m+1/2} \alpha^i r^i_{m+1/2} \\ &= f - df^{i+}, \end{aligned} \tag{19}$$

in which:

$$\alpha^i_{m+1/2} = \ell^i_{m+1/2}(Q_{m+1} - Q_m),$$

and:

$$df^{i\pm}_{m+1/2} = \lambda^{i\pm}_{m+1/2} \alpha^i_{m+1/2} r^i_{m+1/2}.$$

VISCOUS TERMS

In this section, the discretization of viscous terms in the TLNS equations are explained.

Table 1. The left and right eigenvectors of Jacobian matrix.

$\ell^1 = \left\{ \left[\frac{\gamma-1}{c}\right]/\sqrt{2}, \left[\frac{\gamma-1}{c}\theta + \hat{n}_x u + \hat{n}_y v + \hat{n}_z w\right]/\sqrt{2}, \left[-\frac{\gamma-1}{c}u - \hat{n}_x\right]/\sqrt{2}, \left[-\frac{\gamma-1}{c}v - \hat{n}_y\right]/\sqrt{2}, \left[-\frac{\gamma-1}{c}w - \hat{n}_z\right]/\sqrt{2} \right\}$	$r^1 = \left\{ \left[\frac{\theta}{c} + \frac{c}{\gamma-1} - \hat{n}_x u - \hat{n}_y v - \hat{n}_z w\right]/\sqrt{2}, \left[\frac{1}{c}\right]/\sqrt{2}, \left[\frac{u}{c} - \hat{n}_x\right]/\sqrt{2}, \left[\frac{v}{c} - \hat{n}_y\right]/\sqrt{2}, \left[\frac{w}{c} - \hat{n}_z\right]/\sqrt{2} \right\}$
$\ell^2 = \left\{ -\frac{\gamma-1}{c}\hat{n}_y, -\frac{\gamma-1}{c}\hat{n}_y\theta + \hat{n}_y c - \hat{n}_z u + \hat{n}_x w, \frac{\gamma-1}{c}\hat{n}_y u + \hat{n}_z, \frac{\gamma-1}{c}\hat{n}_y v, \frac{\gamma-1}{c}\hat{n}_y w + \hat{n} \right\}$	$r^2 = \left\{ \frac{\theta}{c}\hat{n}_y + \hat{n}_z u - \hat{n}_x w, \frac{\hat{n}_y}{c}, \frac{u}{c}\hat{n}_y + \hat{n}_z, \frac{v}{c}\hat{n}_y, \frac{w}{c}\hat{n}_y - \hat{n}_x \right\}$
$\ell^3 = \left\{ -\frac{\gamma-1}{c}\hat{n}_z, -\frac{\gamma-1}{c}\hat{n}_z\theta + \hat{n}_z c + \hat{n}_y u - \hat{n}_x v, \frac{\gamma-1}{c}\hat{n}_z u - \hat{n}_y, \frac{\gamma-1}{c}\hat{n}_z v + \hat{n}_x, \frac{\gamma-1}{c}\hat{n}_z w \right\}$	$r^3 = \left\{ \frac{\theta}{c}\hat{n}_z - \hat{n}_y u + \hat{n}_x v, \frac{\hat{n}_z}{c}, \frac{u}{c}\hat{n}_z - \hat{n}_y, \frac{v}{c}\hat{n}_z + \hat{n}_x, \frac{w}{c}\hat{n}_z \right\}$
$\ell^4 = \left\{ -\frac{\gamma-1}{c}\hat{n}_x, -\frac{\gamma-1}{c}\hat{n}_x\theta + \hat{n}_x c + \hat{n}_z v - \hat{n}_y w, \frac{\gamma-1}{c}\hat{n}_x u, \frac{\gamma-1}{c}\hat{n}_x v - \hat{n}_z, \frac{\gamma-1}{c}\hat{n}_x w + \hat{n}_y \right\}$	$r^4 = \left\{ \frac{\theta}{c}\hat{n}_x - \hat{n}_z v + \hat{n}_y w, \frac{\hat{n}_x}{c}, \frac{u}{c}\hat{n}_x, \frac{v}{c}\hat{n}_x - \hat{n}_z, \frac{w}{c}\hat{n}_x + \hat{n}_y \right\}$
$\ell^5 = \left\{ \left[\frac{\gamma-1}{c}\right]/\sqrt{2}, \left[\frac{\gamma-1}{c}\theta - \hat{n}_x u - \hat{n}_y v - \hat{n}_z w\right]/\sqrt{2}, \left[-\frac{\gamma-1}{c}u + \hat{n}_x\right]/\sqrt{2}, \left[-\frac{\gamma-1}{c}v + \hat{n}_y\right]/\sqrt{2}, \left[-\frac{\gamma-1}{c}w + \hat{n}_z\right]/\sqrt{2} \right\}$	$r^5 = \left\{ \left[\frac{\theta}{c} + \frac{c}{\gamma-1} + \hat{n}_x u + \hat{n}_y v + \hat{n}_z w\right]/\sqrt{2}, \left[\frac{1}{c}\right]/\sqrt{2}, \left[\frac{u}{c} + \hat{n}_x\right]/\sqrt{2}, \left[\frac{v}{c} + \hat{n}_y\right]/\sqrt{2}, \left[\frac{w}{c} + \hat{n}_z\right]/\sqrt{2} \right\}$

Viscous terms in the TLNS equations are expressed as:

$$\tilde{F}_v = \frac{\eta_x}{J}E_v + \frac{\eta_y}{J}F_v + \frac{\eta_z}{J}G_v. \tag{20}$$

Considering Relations 3 and 4, it is obvious that the stress tensors should be computed. Computation of stresses using the finite volume method in a given cell is done by applying the divergence theorem. Let Ω be an arbitrary volume and S be the closed boundary surface of the cell, therefore:

$$\int_\Omega \vec{\nabla} U d\Omega = \oint_S U d\vec{S}. \tag{21}$$

The average velocity gradients are defined as:

$$\begin{aligned}
\left(\overline{\frac{\partial u}{\partial x}}\right)_\Omega &= \frac{1}{\Omega}\int_\Omega \frac{\partial u}{\partial x}d\Omega = \frac{1}{\Omega}\oint U dS_x \\
&= \frac{1}{\text{vol}}\sum U_{nb}(n_x)_{nb} \\
&= \frac{1}{\text{vol}}\Bigg\{ U_{j+1/2,k,i}\cdot\left(\frac{\xi_x}{J}\right)_{J+1/2,k,i} \\
&\quad - U_{j-1/2,k,i}\cdot\left(\frac{\xi_x}{J}\right)_{J-1/2,k,i} \\
&\quad + U_{j,k+1/2,i}\cdot\left(\frac{\eta_x}{J}\right)_{J,k+1/2,i} \\
&\quad - U_{j,k-1/2,i}\cdot\left(\frac{\eta_x}{J}\right)_{J,k-1/2,i} \\
&\quad + U_{j,k,i+1/2}\cdot\left(\frac{\zeta_x}{J}\right)_{J,k,i+1/2} \\
&\quad - U_{j,k,i-1/2}\cdot\left(\frac{\zeta_x}{J}\right)_{J,k,i-1/2}\Bigg\},
\end{aligned} \tag{22}$$

$$\begin{aligned}
\left(\overline{\frac{\partial u}{\partial x}}\right)_\Omega &= \frac{1}{\Omega}\int_\Omega \frac{\partial u}{\partial y}d\Omega = \frac{1}{\Omega}\oint U dS_y \\
&= \frac{1}{\text{vol}}\sum U_{nb}(n_y)_{nb} \\
&= \frac{1}{\text{vol}}\Bigg\{ U_{j+1/2,k,i}\cdot\left(\frac{\xi_y}{J}\right)_{J+1/2,k,i} \\
&\quad - U_{j-1/2,k,i}\cdot\left(\frac{\xi_y}{J}\right)_{J-1/2,k,i} \\
&\quad + U_{j,k+1/2,i}\cdot\left(\frac{\eta_y}{J}\right)_{J,k+1/2,i} \\
&\quad - U_{j,k-1/2,i}\cdot\left(\frac{\eta_y}{J}\right)_{J,k-1/2,i} \\
&\quad + U_{j,k,i+1/2}\cdot\left(\frac{\zeta_y}{J}\right)_{J,k,i+\frac{1}{2}} \\
&\quad - U_{j,k,i-1/2}\cdot\left(\frac{\zeta_y}{J}\right)_{J,k,i-1/2}\Bigg\}.
\end{aligned} \tag{23}$$

The other derivatives ($\partial u/\partial z, \cdots$) are discretized in the same way.

ALGEBRAIC MODEL OF TURBULENCE

There are many turbulence models to simulate a turbulent boundary layer, but a useful and simple model, which is examined in many computer assessments and needs less amount of computer time, has been offered by Baldwin and Lomax [11]. This is a zeroth model, in which the effect of turbulence is simulated in terms of an eddy viscosity coefficient (μ_t). Thus, in stress terms of the laminar Navier-Stokes equations, the molecular coefficient of viscosity, (μ), is replaced by ($\mu + \mu_t$). In heat flux terms (K/Cp = μ/Pr) is replaced by (μ/Pr+μ_t/Pr$_t$).

The Baldwin-Lomax model is patterned after an algebraic model developed by Cebeci et al. [14]. This turbulence model is named as a two-layer zeroth equation model and shows that the turbulent flow is divided into an inner and an outer region. A different set of equations is used in each region to determine the turbulent eddy viscosity, μ_t. The final value of μ_t is defined as:

$$\mu_t = \min\Big[(\mu_t)_{\text{inner}}, (\mu_t)_{\text{outer}}\Big]. \tag{24}$$

For the inner layer, the Prandtl-Van Driest formula is used to determine μ_t (the eddy viscosity coefficient), which is defined by:

$$(\mu_t)_{\text{inner}} = \rho l^2 |\Omega|, \tag{25}$$

where l, the mixing length, is given as:

$$l = ky\big[1 - \exp(-y^+/A^+)\big], \tag{26}$$

where k and A^+ are constant and equal to 0.41 and 26, respectively, $|\Omega|$ is the magnitude of the local vorticity vector and is defined as:

$$|\Omega| = \sqrt{\left(\frac{\partial u}{\partial y} - \frac{\partial v}{\partial x}\right)^2 + \left(\frac{\partial v}{\partial z} - \frac{\partial w}{\partial y}\right)^2 + \left(\frac{\partial w}{\partial x} - \frac{\partial u}{\partial z}\right)^2}, \tag{27}$$

and:

$$y^+ = \frac{\sqrt{\rho_w \tau_w}}{\mu_w}y, \tag{28}$$

where, ρ_w, τ_w and μ_w are the density, shear stress and viscosity coefficient at the wall, respectively, and y

is the normal distance from the wall. In the outer region, for attached boundary layers, the turbulent eddy viscosity, (μ_t), is defined as:

$$(\mu_t)_{\text{outer}} = \text{KC}_{\text{cp}}\rho F_{\text{wake}} F_{\text{Kleb}}(y), \tag{29}$$

where K and C_{CP} are constant and equal to 0.0168 and 1.6, respectively and $F_{\text{Kleb}}(y)$ is the Klebanoff intermittence factor;

$$F_{\text{Kleb}} = \left[1 + 5.5\left(\frac{\text{C}_{\text{Kleb}} y}{y_{\max}}\right)^6\right]^{-1}, \tag{30}$$

and:

$$F_{\text{wake}} = \min . \begin{cases} y_{\max} F_{\max} \\ C_{\text{wk}} y_{\max} u^2_{\text{Diff}} / F_{\max} \end{cases}, \tag{31}$$

where C_{kleb} is the Klebanoff constant and equal to 0.3, C_{wk} is the wake constant and equal to 0.25 and:

$$U_{\text{Diff}} = \left(\sqrt{u^2+v^2+w^2}\right)_{\max} - \left(\sqrt{u^2+v^2+w^2}\right)_{\min}. \tag{32}$$

$F_{\max}$ and $y_{\max}$ are determined from the following function:

$$F(y) = y|\Omega|\left[1 - \exp(-y^+/A^+)\right], \tag{33}$$

such that the peak value of $F(y)$ between the wall and the flow field is defined as $F_{\max}$ and the value of y at which this occurs is defined as $y_{\max}$.

TURBULENT MODIFICATION FOR BALDWIN-LOMAX MODEL

A problem with Baldwin-Lomax model is encountered when it is applied to treat flow about slender bodies at incidence [15]. In the separated flow region, it becomes difficult to determine the correct value of $F_{\max}$, which is necessary for evaluation of $\mu_{t,\text{outer}}$. In an attached flow, there is only one maximum for $F(y)$ in the radial direction and $F_{\max}$ is simply determined. When separated flow occurs, two maxima for $F(y)$ are encountered. The first peak occurs in the boundary layer and a second layer peak exists, due to the presence of a vortex sheet. If Baldwin-Lomax model is used to obtain $F_{\max}$, the second maximum in $F(y)$ is obtained. This results in values of $\mu_{t,\text{outer}}$ that are too high, resulting in distortion or a washout of the features in the computed flow [15]. A modification to Baldwin-Lomax model has been proposed by Degani and Schiff and applied by Weinacht et al. [12]. For each axial station, a maximum value of the scaling length, $y_{\max}$, is defined as 1.8 times the value of $y_{\max}$ on the windward ray for non-spinning bodies. A peak in $F(y)$ is defined if the value of $F(y)$ drops below 90% of the local maximum. Where two separate distinct peaks in $F(y)$ exist, the peak closer to the body is chosen. If the two peaks in $F(y)$ merge into one abnormally large peak (or a peak cannot be found at all), the value of $F_{\max}$ is frozen at the value used for the previous roll angle.

EXPLICIT SOLUTION PROCEDURE

In this section, an explicit method is considered and discussed. The conservative form of the TLNS equations is discretized in the following form:

$$\frac{\hat{Q}^{n+1} - \hat{Q}^n}{\Delta\tau} + \left(\hat{E}_{j+1/2,k,l} - \hat{E}_{j-1/2,k,l}\right)^n + \left(\left(\hat{F}-\hat{F}_v\right)_{j,k+1/2,l} - \left(\hat{F}-\hat{F}_v\right)_{j,k-1/2,l}\right)^n + \left(\hat{G}_{j,k,l+1/2} - \hat{G}_{j,k,l-1/2}\right)^n = 0. \tag{34}$$

Therefore:

$$\hat{Q}^{n+1} = \hat{Q}^n - \Delta\tau\left\{\left(\hat{E}_{j+1/2,k,l} - \hat{E}_{j-1/2,k,l}\right)^n + \left((\hat{F}-\hat{F}_v)_{j,k+1/2,l} - (\hat{F}-\hat{F}_v)_{j,k-1/2,l}\right)^n + \left(\hat{G}_{j,k,l+1/2} - \hat{G}_{j,k,l-1/2}\right)^n\right\}. \tag{35}$$

The solution of the system of equations with the above procedure is straightforward and this procedure is repeated until the flow field is steady, that is, the residue ($R = \sum_{m=i,j,k} \rho_m^{n+1} - \rho_m^n$) decreases less than a desired number.

GRID GENERATION

The grid generation is performed in two steps. In the first, a few 2-D grids of O type are generated at different cross-flow planes. In the second step, these 2-D grids are connected to make a 3-D grid. The outer radius of the grids is obtained using the Taylor-Makcoll solution around the nose of the ogive to include the outer shock. A circumferential plane and a cross-flow plane of a generated grid for a secant-ogive with an incidence angle of 10° are shown in Figure 2.

RESULTS AND DISCUSSION

Figures 3 to 6 show circumferential pressure distribution in different axial sections for a supersonic flow

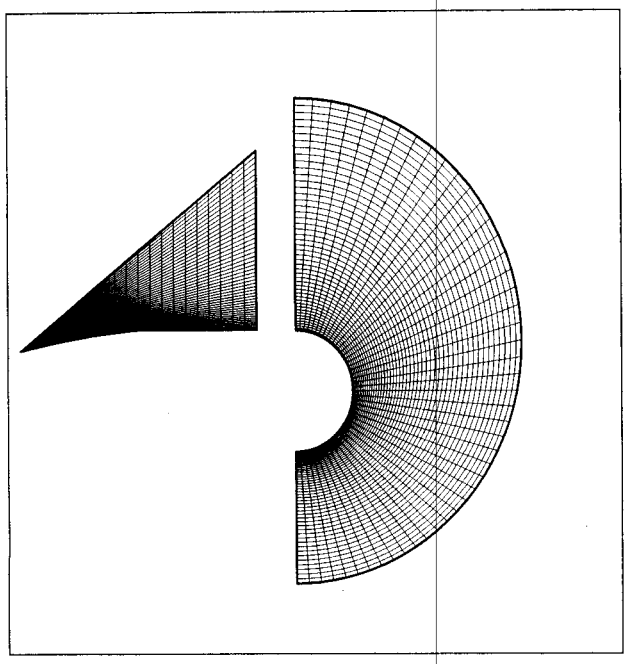

Figure 2. Axial and circumferential sections of generated grid for a secant-ogive with incidence angle of 10°.

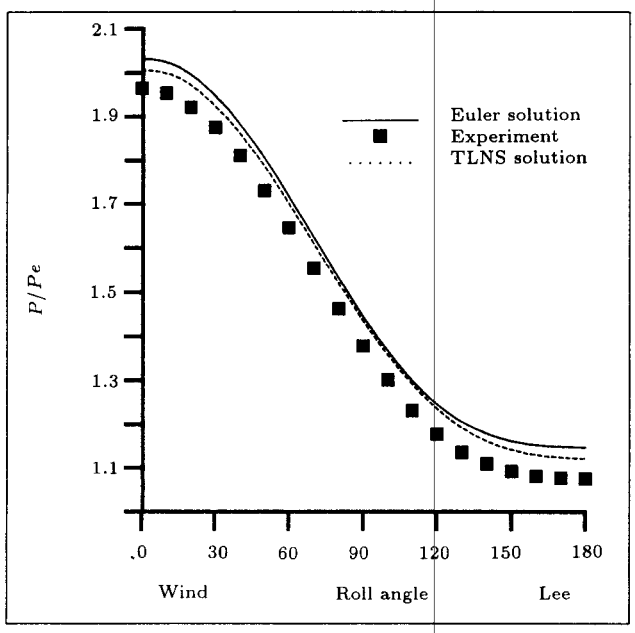

Figure 3. The comparison of pressure, α=6, Mach number = 3 and $x/D = 1.57$.

with Mach number of 3 and $\mathrm{Re}_\infty = 4.101 \times 10^6/\mathrm{m}$ past a tangent-ogive. The incidence angle is 6°. The numerical results are compared with experiments [16] and Euler solution results. Because of the cross flow separation at $x/D > 3$, the accuracy of results in the leeward region is decreased. As expected, TLNS results are more exact than Euler results.

Figures 7 to 10 show circumferential pressure

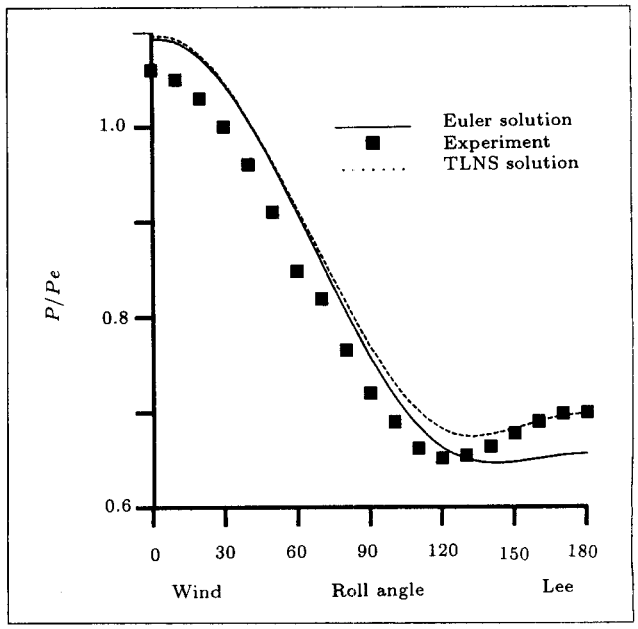

Figure 4. The comparison of pressure, α=6, Mach number = 3 and $x/D = 3.13$.

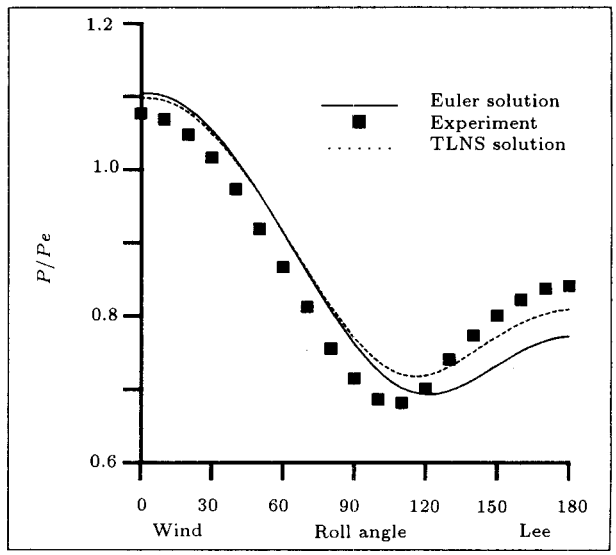

Figure 5. The comparison of pressure, α=6, Mach number = 3 and $x/D = 4.14$.

distribution in different axial sections for a supersonic flow with Mach number of 3 and $\mathrm{Re}_\infty = 4.101 \times 10^6/\mathrm{m}$ past a secant-ogive. The incidence angle is 10°. The numerical results are compared with experiments [16] and Euler solution results. Due to the higher incidence angle, the separation zone is bigger in comparison with the incidence angle of 6°. Also, a supersonic cross-flow occurred in this case and the interaction of this shock with the viscous layer creates a complex flow.

In Figure 11, the axial distribution of pressure at the windward and leeward angle is presented. An expansion is captured at $x/D = 3$, in which the ogive

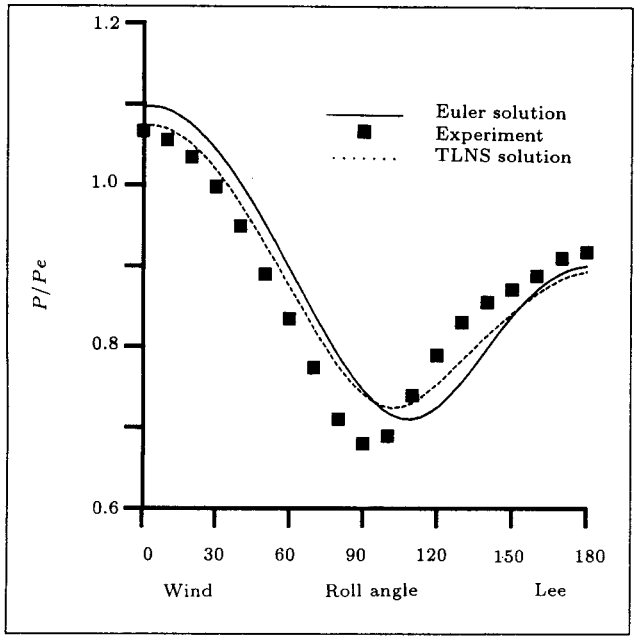

Figure 6. The comparison of pressure, α=6, Mach number = 3 and $x/D = 5.77$.

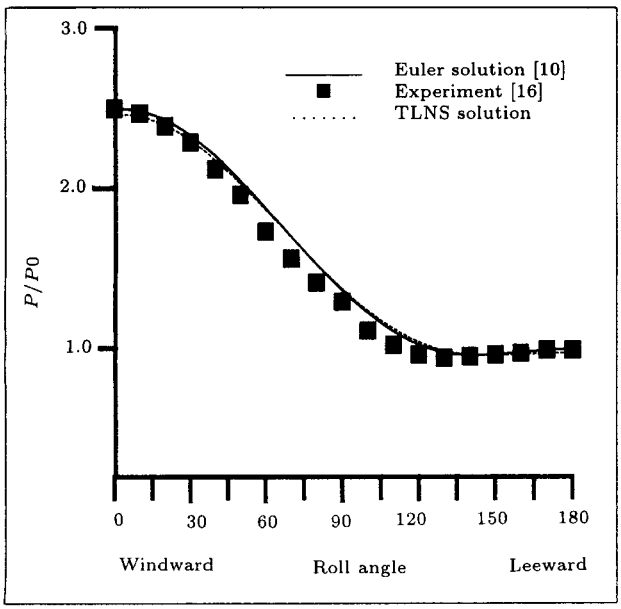

Figure 7. The comparison of pressure, α=10, Mach number = 3 and $x/D = 1.56$.

section is connected to the cylindrical section. This phenomenon appeared in experiments also.

In Figure 12, cross-flow tangential velocity contours are shown. A cross-flow separation zone is captured in the leeward region. The interaction of this zone with the supersonic cross-flow changes the usual pressure distribution about secant-ogive at the incidence angle of 10°(Figure 10). Figure 13 shows this accelerated supersonic cross-flow.

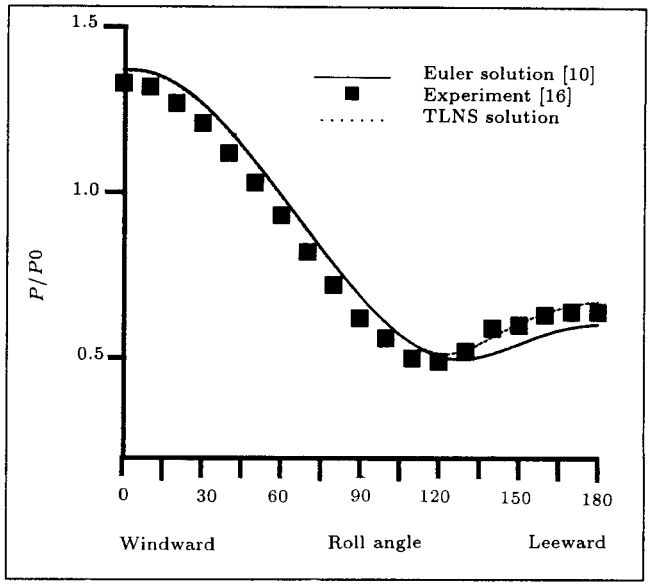

Figure 8. The comparison of pressure, α=6, Mach Number = 3 and $x/D = 3.13$.

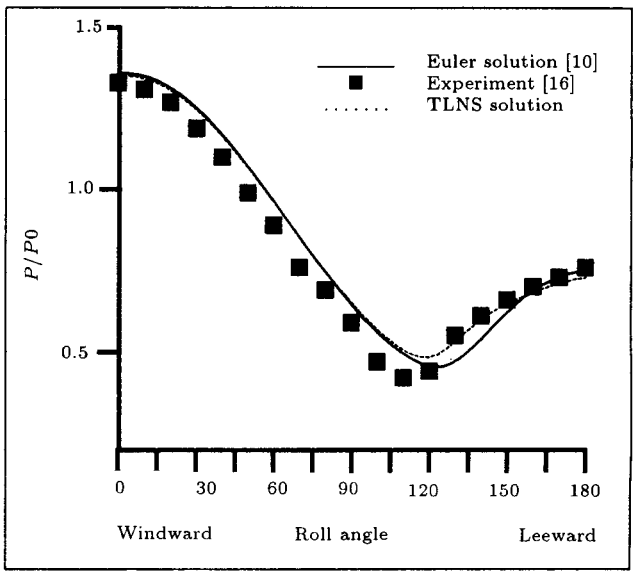

Figure 9. The comparison of pressure, α=10, Mach number = 3 and $x/D = 4.14$.

ACKNOWLEDGMENT

The authors wish to thank the Research Council of Iran for their support provided under grant # 1098.

NOMENCLATURE

C	speed of sound
E	total energy
E, F, G	inviscid fluxes
E_v, F_v, G_v	viscous fluxes
$\tilde{E}, \tilde{F}, \tilde{G}$	fluxesin general curvilinear coordinates

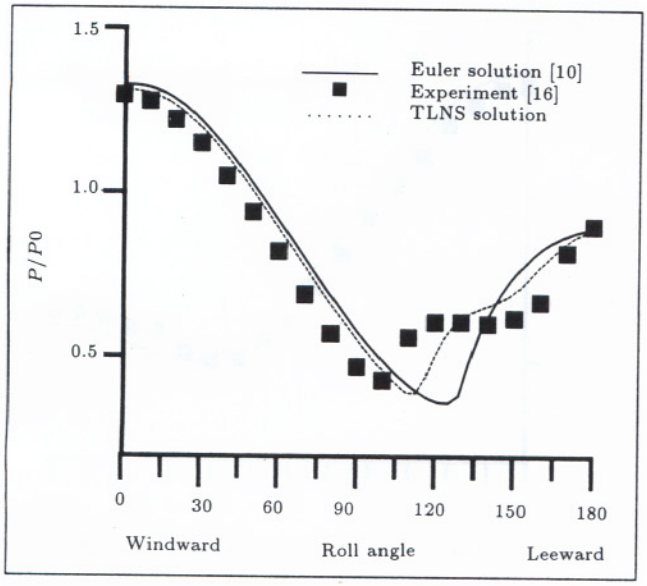

Figure 10. The comparison of pressure, α=10, Mach number = 3 and $x/D = 5.77$.

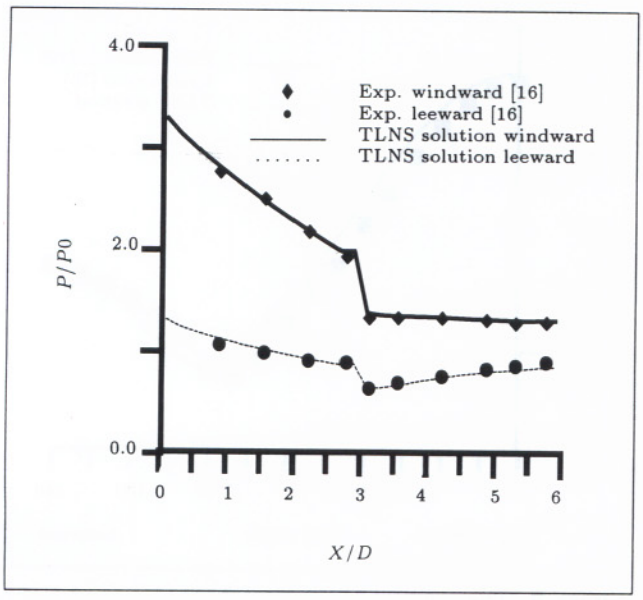

Figure 11. Axial distribution of pressure at windward and leeward angle, $\alpha = 10$, Mach number = 3.

F_{Kleb}	Klebanoff intermittence factor
F_{Wake}	wake function
J	Jacobian of transformation
H	enthalpy
K	thermal conductivity
n_x, n_y, n_z	components of surface vector
q_x, q_y, q_z	heat conduction terms
Q	primitive variable matrix
P	pressure
Pr	Prandtl number
r^I	right eigen vector

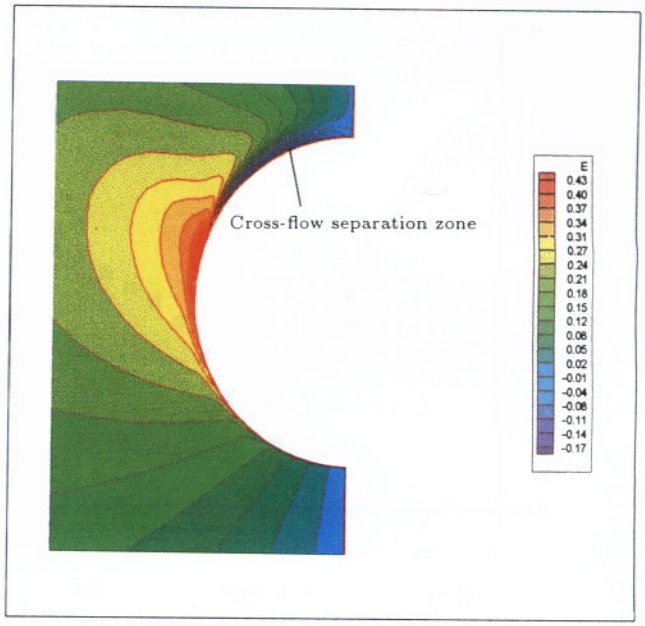

Figure 12. Cross-flow tangential velocity contours, $\alpha = 10$, Mach number = 3 and $x/D = 5.77$.

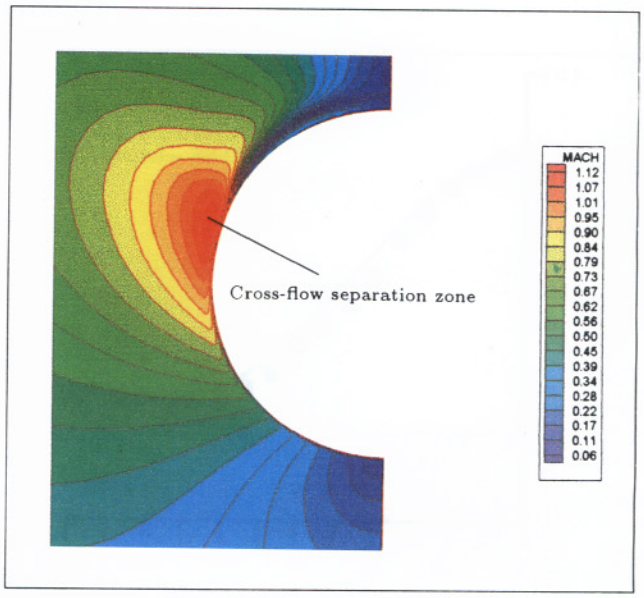

Figure 13. Cross-flow Mach number contours, $\alpha = 10$, Mach number = 3 and $x/D = 5.77$.

T	temperature
u, v, w	velocities
V	volume
x, y, z	coordinates of Cartesian.

Greek Symbols

Ω	volume of the element
λ	eigenvalue
μ	viscosity coefficient
μ_t	turbulent viscosity coefficient

10-4

ρ specific mass

τ_{ij} tensor of stresses

ξ, η, ζ general curvilinear coordinates

ℓ^i left eigenvector.

$(\frac{\xi_{x,y,z}}{J})_{j+1/2}$, $(\frac{\eta_{x,y,z}}{J})_{k+1/2}$, $(\frac{\zeta_{x,y,z}}{J})_{i+1/2}$ metrices and components of surface vector.

REFERENCES

1. Lax, P.D. and Wendroff, B. "System of conservation laws", *Comm. Pure Apple. Math.*, **13**, pp 217-237 (1960).
2. MacCormack, R.W. "The effect of viscosity in hypervelocity impact cratering", *AIAA*, paper 69-354, Cincinnati, Ohio (1969).
3. Godonov, S.K. "A difference scheme for numerical computation of discontinuous solution of hydrodynamic Equations", *Math. Sbornic*, **47**, pp 271-306 (in Russian), Translated US Joint Publ. Res. Service, JPRS 7226 (1969).
4. Osher, S. "Numerical solution of singular perturbation problems and hyperbolic system of conservation laws", O. Axelsson et al., Eds., *Mathematical Studies*, **47**, Amsterdam, North Holland.
5. Roe, P.L. "Approximate Riemann solvers, parameter vectors and difference schemes", *Journal of Computational Physics*, **45** (1981).
6. Edge, H., Sahu, J., Sturek, W. and Behr, M., *Cfd Computations with ZNS Flow CHSSI Software*, Dept. of Defence High Performance Computing Program, User Group Conference (1999).
7. Behr, M., Pressel, D.M. and Sturek, W.B. "Comments on CFD code performance on scalable architectures", *Computer Methods in Applied Mechanics and Engineering*, pp 263-277 (2000).
8. Lawrence, S.L., Chaussee, D.S. and Tannehill, J.C. "Application of an upwind algorithm to the three dimensional parabolized Navier-Stokes equations", *AIAA*, paper 87-1112 (1987).
9. Emdad, H., Alishahi, M.M., Goshtasbi Rad, E. "Computation of high Reynolds number, parabolized Navier-Stokes equations based on upwinding algorithm", *Journal of Scientia Iranica*, Sharif University of Technology, **6**(2) (Spring 1999).
10. Alishahi, M.M., Emdad, H. and Abouali, O. "3-D solution of Euler equations for supersonic flow with Roe method", *Proceeding of AERO 2000*, **1**, pp 181-190.
11. Baldwin, B.S. and Lomax, H. "Thin layer approximation and algebraic for model separated turbulent flow", *AIAA*, paper 78-257, 16th Aerospace Meeting (Jan. 1978).
12. Weinacht, P., Guidos, B.S., Sturek, W.B. and Hodes, B.A. "PNS computations for spinning shell at moderate angle of attack and for long L/D finned projectiles", *AIAA*, Paper No. 85-0273, AIAA 23rd Aerospace Science Meeting (1985).
13. Chackravarthy, S.R. and Szema, K.Y. "Euler solver for three-dimensional supersonic flows with subsonic packets", *Journal of AIRCRAFT*, **24**(2), pp 73-83 (Feb. 1987).
14. Cebeci, T., Smith, A.M.O. and Mosinkis, G. "Calculation of compressible adiabatic turbulent boundary layer", *AIAA Jour.*, **8**(11), pp 1976-1982 (1970).
15. Gee, K., Cummings, R.M. and Schiff, L.B. "Turbulent model effects on separated flow about a prolate spheroid", *AIAA Jour.*, **30**(3), pp 654-664 (March 1992).
16. Raklis, R.P. and Sturek, W.B. "Surface pressure measurements on slender bodies at angle of attack at supersonic speeds", *U.S. Army Ballistic Research Laboratory*, Aberdeen Proving Ground, Maryland ARBRL-MR-02876 (AD A064097) (Nov. 1978).